Lithos 127 (2011) 323–335

Contents lists available at SciVerse ScienceDirect

Lithos

journal homepage: www.elsevier.com/locate/lithos

Chalcophile elemental constraints on sulfide-saturated fractionation of Cenozoic basalts and andesites in SE China

Alexandra Yang Yang [a,b,c], Tai-Ping Zhao [a,b,*], Liang Qi [d], Sheng-Hong Yang [d], Mei-Fu Zhou [d]

[a] Key Laboratory of Mineralogy and Metallogeny, Guangzhou Institute of Geochemistry, Chinese Academy of Sciences, Guangzhou 510640, China
[b] Key Laboratory of Marine Hydrocarbon Resources and Environmental Geology, Ministry of Land and Resources, Qingdao 266061, China
[c] Graduate University of Chinese Academy of Sciences, Beijing 100039, China
[d] Department of Earth Sciences, The University of Hong Kong, Pokfulam Road, Hong Kong SAR, China

ARTICLE INFO

Article history:
Received 15 April 2011
Accepted 25 August 2011
Available online 3 September 2011

Keywords:
Cenozoic
Basalt
Andesite
Platinum-group elements
SE China

ABSTRACT

Cenozoic volcanic rocks are widespread in eastern China. These rocks have variable isotope compositions, reflecting different mantle sources under SE and NE China. In order to explore their PGE variations, chalcophile elements are determined for basalts from Leiqiong and Sanshui and andesites from Lianping in SE China. Basalts from Leiqiong have higher Ni (66–376 ppm) and Cu (30–73 ppm) contents than those from Lianping and Sanshui. All the samples have extremely low PGE contents, low Cu/Zr (<1) and high Cu/Pd ratios (19,000–475,000), except for one olivine-rich sample with much higher PGE concentrations. All the samples have variable Pd/Ir (6.1–185) and Pt/Rh ratios (1.07–43). They are PGE-depleted relatively to Ni and Cu and have U-shaped and MORB-like primitive mantle-normalized chalcophile element patterns. Positive correlations of Ni and Cr with MgO in basalts from Leiqiong suggest fractionation of olivine and chromite. All samples have low Cu/Zr and high Cu/Pd ratios, implying that sulfides were segregated during magmatic evolution. Quantitative modeling indicates that the amounts of sulfide removed from the samples are smaller than that from MORB. Sanshui basalts are depleted in Ru and Pt, indicating fractionation of chromite with Fe–Pt alloys and/or accumulation of olivine with Ir alloys. A few Leiqiong and Lianping andesites may also have experienced fractionation of Fe–Pt alloys based on Pt depletions relative to Rh and Pd. Alternatively, the Pt depletion could also be an inherited feature of a metasomatic mantle source. Basalts from Sanshui have the highest and andesites from Lianping have the lowest Pd/Ir ratios, also consistent with a metasomatized source for the andesites in Lianping.
The volcanic rocks from SE China show no strong Ir-depletions, unlike those from NE China. The absence of strong Ir-depletions is likely due to more oxidized SCLM beneath SE.

1. Introduction

Cenozoic magmatism in the continental margin of eastern China was associated with extensional basins related to the Indo-Asian collision (Liu et al., 2004) and/or subduction of the Paleo-Pacific Plate (Northrup et al., 1995). The volcanic rocks are predominantly basalts and are thought to have been derived from variable mantle sources (Chung et al., 1994; Fan and Hooper, 1991; Zhou and Armstrong, 1982; Zou et al., 2000). It is commonly accepted that basalts in SE China originated from a mixed source involving asthenospheric mantle and EM2, and that those in NE China were derived from a mixed source of asthenospheric mantle and EM1 (e.g. Ho et al., 2000; Zou et al., 2000; Han et al., 2009).

Platinum-group elements (PGEs) are sensitive to sulfide saturation and silicate fractionation (e.g., Barnes et al., 1985; Barnes and Picard, 1993; Brügmann et al., 1987) and provide a powerful tool for examining the petrogenesis of mafic rocks (e.g., Keays, 1995; Lightfoot and Keays, 2005; Wang et al., 2011; Zhou, 1994). Chu et al. (1999) determined the concentrations of PGEs of basalts and peridotite xenoliths from Hannuoba, NE China, and reported an extreme depletion of Ir relative to other PGEs (Fig. 5d). Ir-depleted mantle xenoliths have also been found elsewhere in NE China (Orberger et al., 1998; Xu et al., 1998; Zheng et al., 2005). Such Ir depletion is thus thought to be a feature of the upper mantle in eastern China (Chu et al., 1999; Orberger et al., 1998). However, mantle xenoliths found in Nushan, Anhui Province (SE China), show PGE patterns without significant Ir depletions (Liu et al., 2010). Because no PGE data are currently available on the volcanic rocks of SE China, it is unknown whether partial melting of different mantle sources would produce melts with different PGE characteristics and whether the petrogenesis of the volcanic rocks in SE and NE China is comparable.

The Leiqiong (Leizhou Pennisula and Hainan Island) volcanic field has the largest exposure of Cenozoic basalts in SE China, representing the most recent volcanism in the region (Fig. 1). On the other hand, basalts and andesites in the Sanshui and Lianping basins of the

* Corresponding author at: Key Laboratory of Mineralogy and Metallogeny, Guangzhou Institute of Geochemistry, Chinese Academy of Sciences, Guangzhou 510640, China. Tel.: +86 20 85290231; fax: +86 20 85290130.
E-mail address: tpzhao@gig.ac.cn (T.-P. Zhao).

0024-4937/$ – see front matter © 2011 Elsevier B.V. All rights reserved.
doi:10.1016/j.lithos.2011.08.016

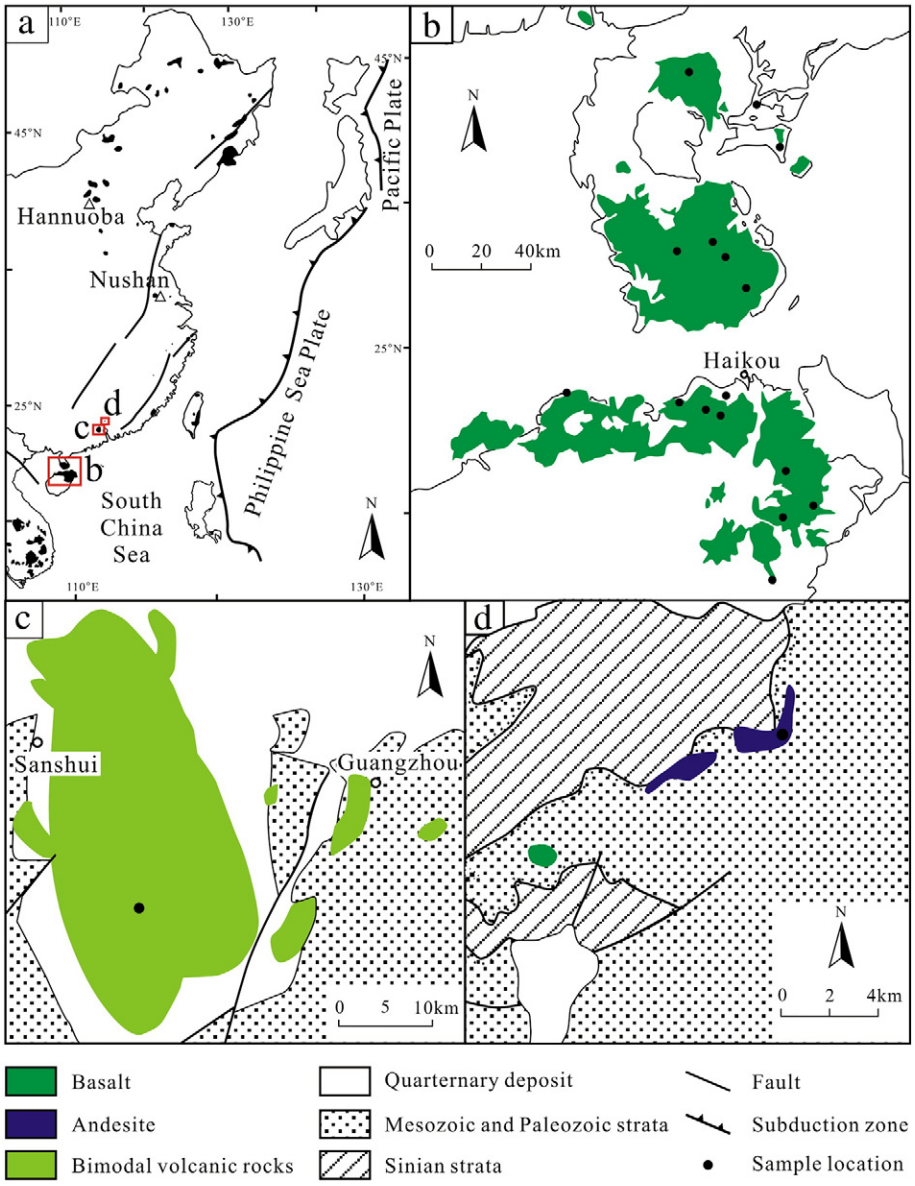

Fig. 1. a. Sketch map showing outcrops of Cenozoic volcanic rocks in eastern China, modified from the geological map of China. Rectangles mark the regions studied; b) Leiqiong area; c) Sanshui basin; d) Lianping basin. Simplified geologic maps and sampling locations of Cenozoic volcanic rocks from the three localities are shown in b, c and d.

Guangdong Province mark the beginning of Cenozoic volcanism in SE China. This paper presents new PGE data for Neogene basalts from Leiqiong and Paleogene basalts and andesites from Sanshui and Lianping. The aim of this study is to examine the roles of fractionation and sulfide saturation in the genesis of these volcanic rocks. This study has significant bearings on the mantle sources for Cenozoic volcanic rocks in SE and NE China.

2. Geological background

Eastern China is situated in the easternmost part of the Eurasian Plate. In the early Cretaceous, when the Pacific and Philippine Plates were a single continuous feature (Hilde et al., 1977), the Paleo-Pacific Plate was subducted beneath eastern China (Uyeda and Miyashiro, 1974) and back-arc spreading locally transformed the continental crust in eastern China into oceanic crust (Cong et al., 1979).

The Cenozoic extensional basins in eastern China are the surface expressions of shallow mantle dynamics in the region, linked to the Indo-Asian collision (Liu et al., 2004) and/or the rollback of the subducting Paleo-Pacific Plate (Northrup et al., 1995). By the Paleogene, a series of NE-trending fractures was activated in the north, accompanying the opening of the South China Sea in the south. Thereafter, extensive volcanism took place in NE China and in the vicinity of the South China Sea (Fig. 1).

3. Field relations and petrography

In the Leiqiong area, Cenozoic basalts crop out over an area of ~7000 km^2 with the thickness up to 224 m (GBGMR, 1988). The early volcanism (5.6–0.8 Ma) produced predominantly tholeiitic basalts, followed by a later phase (<0.8 Ma) composed of alkali and tholeiitic basalts (Ho et al., 2000; Zhou et al., 1988). All types are porphyritic, containing phenocrysts of plagioclase and clinopyroxene ± olivine. Most of the rocks are fresh with only minor alteration of olivine to iddingsite. A few samples contain olivine xenocrysts (<0.1 wt.% CaO, high Fo ~90) (Fig. 2a and b) and peridotite xenoliths. Magnetite is a ubiquitous minor mineral. Detailed petrological characteristics are described in Han et al. (2009).

To the northeast of Leiqiong are the Sanshui and Lianping basins bounded by NE-trending faults and containing Paleogene volcanic

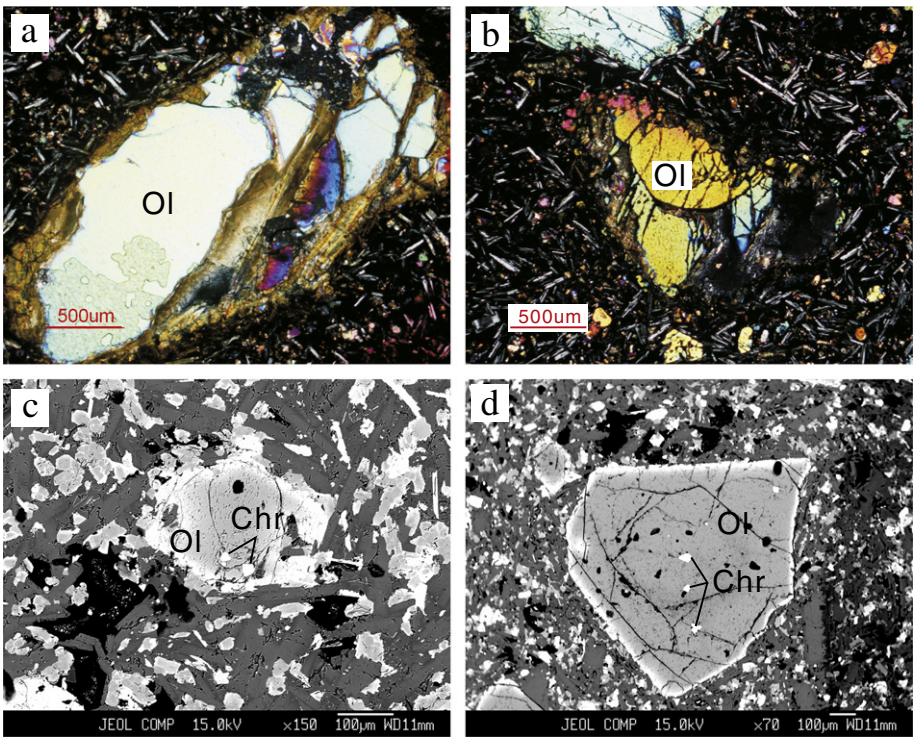

Fig. 2. Photomicrographs of volcanic rocks from SE China: a and b. a basalt (HWGA) showing a large olivine xenocrysts (Fo ~90, CaO<0.1%), under plane-polarized light. c and d. BSE imagines of two basalts (sample HHLA and SY9) showing olivine phenocrysts and euhedral chromite inclusions in olivine grains. Abbreviations: Ol — olivine; Chr — chromite.

rocks (43–60 Ma, Zhou et al., 2009). Bimodal volcanic rocks in the Sanshui basin, including basalts, trachytes, rhyolites and corresponding pyroclastic rocks, crop out over an area of about 3300 km² with an average thickness of 2.8 km (GBGMR, 1988; Zhang et al., 1993). The basalts are porphyritic rocks containing subhedral to euhedral phenocrysts of plagioclase (An_{32-69}), olivine (Fo_{70-85}) and clinopyroxene (En_{64-76}). Most of the rocks are fresh, although clinopyroxene phenocrysts may be partly altered to chlorite. The fine-grained groundmass is composed of plagioclase, clinopyroxene, olivine, magnetite and interstitial glass.

Basalts and andesites (~54 Ma, Chung et al., 1997), which form a sequence with a thickness of ca. 150 m, are intercalated with Early Paleogene sedimentary rocks in the center of the Lianping basin (Fig. 1d) (GBGMR, 1988). The andesites are mainly porphyritic, with euhedral phenocrysts of plagioclase (An_{59-63}) and clinopyroxene (En_{62-74}). They are set in an intersertal matrix composed mostly of plagioclase, clinopyroxene and opaque minerals such as magnetite.

4. Analytical methods

Analyses of major and trace elements including Ni and Cu were performed at the Guangzhou Institute of Geochemistry, Chinese Academy of Sciences. The major elements were analyzed by XRF and the trace elements by ICP-MS. The analytical uncertainties are ±1–2% for major element oxides, ±5% for rare-earth elements, and ±5–10% for other trace elements. Detailed analytical procedures are given in Liu et al. (1996).

PGE concentrations were measured by isotope dilution (ID)-ICP-MS after digestion of samples using a Carius tube technique in the State Key Lab of Ore Deposit Geochemistry, Institute of Geochemistry, Chinese Academy of Sciences, Guiyang. Eight grams of rock powder and an appropriate amount of enriched isotope spike solution containing ^{193}Ir, ^{101}Ru, ^{194}Pt and ^{105}Pd were digested with 23 ml aqua regia in a 120-ml pre-cleaned Carius tube, which was then sealed, placed in an oven and heated to 200 °C. After 10 h, the Carius tube was cooled and the contents were transferred to a 50-ml centrifuge tube. After centrifuging, the upper solution was transferred to another 50-ml centrifuge tube, and the residue was transferred to a 125-ml Savillex Teflon beaker, digested with 20-ml HF and evaporated to dryness. Following this, 3 ml of concentrated HCl was added and the solution evaporated to dryness. This procedure was repeated to remove HF from the solution, and then the upper centrifugated liquid was added and dried. In the next step, 6 ml of concentrated HCl was added and evaporated to dryness to clear the solution of HNO_3. The residue was dissolved with 50-ml of 3 N HCl and transferred to a 50-ml tube for centrifuging at 4000 rpm for 5 min. The upper solution was then used to pre-concentrate PGE by Te-coprecipitation following the procedure described by Qi et al. (2004). The total procedural blanks were 0.009 ng for Ir, 0.007 ng for Ru, 0.009 ng for Rh, 0.022 ng for Pt and 0.036 ng for Pd. The detection limits were 0.0024 ppb for Ir, 0.003 ppb for Ru, 0.002 ppb for Rh, 0.005 ppb for Pt and 0.006 ppb for Pd. Analytical results for standard reference materials WGB-1 (gabbro) and TDB-1 (diabase) are shown in Appendix 1. The PGE concentrations for Ru, Rh and Ir in WGB-1 and TDB-1 are lower than the certified values, but agree well with values reported by Meisel and Moser (2004). The analytical uncertainties are within 15% for Ir and Ru, and within 10% for Rh, Pt and Pd.

5. Analytical results

5.1. Major and trace elements

Major and trace element compositions of the volcanic rocks of SE China are given in Table 1 and Appendix 2. Samples from Leiqiong include basalts, basaltic andesites and trachybasalts (Fig. 3). Mafic rocks in Leiqiong mostly range from 46 to 54 wt.% SiO_2, 3.0–6.3 wt.% $K_2O + Na_2O$ and 5.9–10.4 wt.% MgO (Fig. 3 and Table 1). Their chondrite-normalized REE patterns are similar to those of ocean island basalts (OIB), showing strong enrichment in LREE (Fig. 4). They have $^{87}Sr/^{86}Sr$ ratios ranging from 0.703176 to 0.704481 and εNd from +2.5 to +6.0 (Han et al., 2009).

Table 1
Major and trace elements and PGE concentrations of representative samples from SE China.

Locality	Leiqiong											
Sample	HXSF	HXYA	HQBA	HWPB	HWNA	HHJA	HWGA	HHLA	B06	8-1	T-471	R4
Rock type	t. basalt	t. basalt	basalt	b. andesite	basalt	b. andesite	t. basalt	b. andesite	basalt	basalt	basalt	basalt
Oxides (wt.%)												
SiO_2	50	49	51	52	49	54	48	53	51	48	47	50
TiO_2	2.3	2.5	2.0	2.0	1.9	2.0	2.3	2.1	1.6	2.0	1.9	1.5
Al_2O_3	14	14	13	13	14	14	12	14	15	15	14	15
Fe_2O_3	11	11	12	11	11	11	12	11	11	11	11	10
MnO	0.16	0.16	0.16	0.04	0.14	0.15	0.17	0.15	0.14	0.17	0.14	0.14
MgO	6.9	5.9	6.8	7.3	6.5	6.5	10.4	7.5	7.8	7.8	7.9	8.1
CaO	9.1	10.1	8.7	8.4	8.9	8.5	7.5	8.5	8.9	8.7	7.5	7.8
Na_2O	3.8	3.8	3.0	3.5	2.9	3.1	3.3	3.2	3.8	3.4	2.8	3.2
K_2O	2.0	2.5	1.3	0.88	0.43	0.40	2.0	0.81	1.0	1.5	1.1	1.2
P_2O_5	0.25	0.54	0.32	0.25	0.32	0.22	0.63	0.28	0.27	0.39	0.35	0.22
L.O.I	0.41	0.19	2.6	1.3	5.4	0.73	2.0	0.59	0.10	2.8	6.2	2.8
Total	100	100	101	100	100	100	100	100	100	100	100	100
Mg#	59	55	58	61	58	58	67	62	63	62	63	65
Trace elements (ppm)												
Sc	19	18	18	18	19	18	17	19	20	20	19	19
V	180	190	152	134	145	131	139	150	137	167	154	144
Cr	215	182	247	239	192	170	458	192	278	171	187	196
Ni	77	66	181	277	137	140	316	126	221	155	142	161
Cu	30	58	52	54	56	42	41	51	73	63	61	68
Rb	37	48	27	21	9	15	46	22	18	38	24	36
Sr	527	643	374	384	404	296	1029	368	440	527	429	386
Y	19	20	21	18	18	14	21	17	9	19	15	15
Zr	199	231	151	164	134	114	267	140	120	168	168	125
Nb	35	49	26	28	28	14	56	19	24	34	31	22
Ba	421	511	290	231	308	154	562	222	212	359	253	298
La	21	27	22	13	18	6	37	12	7	25	19	19
Ce	42	53	44	26	36	11	70	25	14	47	39	37
Pr	5.3	6.6	5.6	3.2	4.4	1.5	8.8	3.3	1.8	5.5	4.9	4.3
Nd	22	26	23	13	18	7	37	14	8	24	21	17
Sm	5.6	6.1	5.8	3.7	4.4	2.4	7.9	4.1	2.1	5.0	4.8	3.9
Eu	1.9	2.2	2.1	1.6	1.7	1.3	2.6	1.6	1.1	1.8	1.7	1.4
Gd	5.5	5.7	6.0	4.1	4.8	2.9	7.3	4.4	2.3	5.1	4.6	3.8
Tb	0.83	0.82	0.90	0.66	0.73	0.48	1.01	0.72	0.37	0.76	0.70	0.58
Dy	4.5	4.3	4.9	3.6	4.2	2.8	5.0	4.0	2.0	4.2	3.6	3.3
Ho	0.75	0.72	0.84	0.61	0.73	0.50	0.88	0.69	0.37	0.73	0.61	0.58
Er	1.8	1.7	2.0	1.5	1.8	1.3	2.0	1.7	0.91	1.8	1.5	1.4
Tm	0.25	0.23	0.27	0.21	0.24	0.18	0.25	0.23	0.13	0.25	0.19	0.21
Yb	1.5	1.3	1.6	1.2	1.4	1.1	1.5	1.4	0.8	1.5	1.2	1.3
Lu	0.21	0.20	0.23	0.18	0.21	0.17	0.20	0.21	0.12	0.22	0.17	0.19
Hf	4.9	4.7	3.8	3.6	3.4	2.8	6.5	3.6	2.8	4.0	3.9	2.9
Ta	2.2	2.6	1.6	1.6	1.6	0.75	3.8	1.1	1.5	2.3	2.1	1.3
Pb	3.0	3.1	2.9	1.2	2.3	1.2	3.3	2.6	3.0	7.5	2.0	4.5
Th	4.1	4.5	3.6	2.2	3.2	1.3	5.9	2.7	2.0	5.1	2.8	4.5
U	0.99	0.99	0.82	0.54	0.52	0.35	1.27	0.62	0.56	1.13	0.76	0.94
PGE (ppb)												
Ir	0.018	0.011	0.044	0.016	0.060	0.010	0.224	0.012	0.030	0.022	0.030	0.021
Ru	0.022	0.025	0.060	0.030	0.058	0.028	0.349	0.025	0.044	0.035	0.057	0.039
Rh	0.016	0.010	0.035	0.039	0.043	0.009	0.147	0.010	0.013	0.020	0.022	0.024
Pt	0.060	0.077	0.354	0.150	0.325	0.080	0.960	0.057	0.175	0.151	0.170	0.175
Pd	0.414	0.546	0.619	0.550	1.045	0.262	1.797	0.217	0.185	0.724	0.330	0.388
Elemental ratios												
Cu/Pd	72,000	105,000	84,000	98,000	53,000	161,000	23,000	236,000	393,000	87,000	184,000	175,000
Pd/Ir	23	48	14	35	17	27	8	19	6	33	11	18
Pt/Rh	3.7	7.7	10.3	3.8	7.5	9.0	6.5	5.8	13.5	7.5	7.6	7.3

Major and trace element data of the Leiqiong basalts are from Han et al. (2009).
Abbreviations: t. basalt — trachy basalt; b. andesite — basaltic andesite.

Volcanic rocks in Sanshui have relatively constant SiO_2 (45–48 wt.%), $K_2O + Na_2O$ (4.8–5.4 wt.%) and MgO (5.4–6.4 wt.%), are high in TiO_2 (>2.50 wt.%) and show moderate Na_2O/K_2O ratios (2.5–3.6) (Table 1 and Appendix 2). In the TAS diagram, they plot in the fields of basalt and trachybasalt due to their high total alkalis (Fig. 3). All the rocks are moderately enriched in LREE (Fig. 4), and their primitive mantle-normalized spider diagrams show strong negative Pb anomalies and moderate enrichment of Nb and Ta relative to La. All of the samples are characterized by high LILE and HFSE (Fig. 4b).

Only andesites were sampled in Lianping (Fig. 3). They have relatively constant SiO_2 (60–61 wt.%) and $K_2O + Na_2O$ (4.6–5.4 wt.%), and low MgO (2.8–3.1 wt.%), TiO_2 (0.67–0.69 wt.%) and Na_2O/K_2O ratios (1.2–1.5) (Table 1 and Appendix 2). Their chondrite-normalized REE patterns are parallel to those of the Sanshui basalts but with lower total REE concentrations (Fig. 4a). All samples are rich in LILE but poor in HFSE with significant negative Nb–Ta and Ti anomalies in the primitive mantle-normalized spider diagram (Fig. 4b). They also show slight depletion in Zr and Hf and enrichment of Pb and Sr.

Locality	Leiqiong	Sanshui					Lianping					
Sample	R8	SS-25	SS-27	SS-28	SS-29	SS-31	LP-1	LP-2	LP-3	LP-7	LP-8	LP-9
Rock type	basalt	t. basalt	basalt	t. basalt	basalt	basalt	andesite	andesite	andesite	andesite	andesite	andesite
Oxides (wt.%)												
SiO_2	50	45	46	46	47	47	61	61	61	60	61	60
TiO_2	1.4	3.2	2.7	2.7	2.7	2.7	0.67	0.68	0.68	0.69	0.68	0.68
Al_2O_3	14	16	17	17	16	16	17	17	17	17	17	17
Fe_2O_3	11	11	11	11	11	11	5	5	6	6	5	6
MnO	0.15	0.15	0.16	0.15	0.15	0.15	0.10	0.10	0.11	0.10	0.11	0.11
MgO	8.1	6.4	5.6	5.5	5.6	5.4	2.8	2.9	3.0	3.1	3.0	3.0
CaO	7.0	9.2	9.0	9.4	9.0	8.8	6.0	6.0	6.0	5.6	6.0	5.9
Na_2O	3.2	3.6	3.9	3.6	4.0	4.0	2.8	2.8	2.7	2.8	2.6	2.8
K_2O	1.5	1.3	1.2	1.2	1.1	1.2	2.3	2.1	2.1	2.2	2.2	2.1
P_2O_5	0.34	0.80	0.94	0.92	0.92	0.93	0.40	0.41	0.41	0.41	0.41	0.41
L.O.I	3.8	2.9	2.0	2.7	2.2	2.7	1.0	1.5	1.4	1.8	1.6	1.7
Total	101	100	99	100	100	100	99	100	100	100	100	100
Mg#	62	57	55	54	55	54	55	56	56	57	56	56
Trace elements (ppm)												
Sc	18	24	19	20	19	19	11	11	10	11	11	11
V	153	239	200	199	199	158	95	94	89	95	94	96
Cr	156	54	57	58	53	50	34	34	33	33	30	31
Ni	133	58	55	57	56	45	18	19	16	19	18	18
Cu	61	40	36	32	36	30	19	14	13	11	11	14
Rb	39	62	76	86	74	33	69	71	70	75	68	67
Sr	492	834	836	1067	878	845	683	742	701	729	702	706
Y	15	28	29	29	29	29	16	16	16	16	17	16
Zr	155	259	293	300	300	237	113	116	118	118	117	115
Nb	31	64	75	77	75	59	10	10	10	10	10	10
Ba	321	688	742	758	760	680	770	746	752	772	748	762
La	19	43	49	51	49	49	33	32	33	33	33	33
Ce	37	81	93	93	92	101	60	61	61	64	60	60
Pr	4.5	10.2	11.2	11.4	11.1	11.4	7.3	7.4	7.4	7.5	7.3	7.4
Nd	18	40	44	44	44	44	28	28	28	28	27	27
Sm	4.3	8.2	8.5	8.4	8.5	8.5	4.8	4.8	4.9	4.9	4.8	4.8
Eu	1.5	2.7	2.7	2.7	2.7	2.6	1.5	1.5	1.5	1.5	1.5	1.5
Gd	4.1	8.0	7.9	7.8	8.2	7.9	4.3	4.2	4.2	4.3	4.3	4.2
Tb	0.61	1.15	1.12	1.15	1.16	1.16	0.58	0.60	0.58	0.59	0.59	0.58
Dy	3.2	5.8	5.9	6.0	5.8	6.0	3.1	3.1	3.1	3.1	3.1	3.0
Ho	0.56	1.09	1.14	1.13	1.14	1.15	0.63	0.61	0.62	0.63	0.64	0.61
Er	1.3	2.8	2.9	2.9	2.8	3.0	1.7	1.7	1.7	1.7	1.7	1.6
Tm	0.19	0.38	0.39	0.40	0.40	0.40	0.24	0.24	0.25	0.25	0.25	0.24
Yb	1.1	2.4	2.6	2.5	2.5	2.6	1.6	1.6	1.6	1.7	1.7	1.6
Lu	0.16	0.36	0.38	0.38	0.36	0.39	0.26	0.25	0.25	0.26	0.26	0.25
Hf	3.2	5.8	6.7	6.8	6.4	5.5	3.1	3.1	3.1	3.3	3.1	3.1
Ta	1.7	3.6	4.9	4.9	4.6	3.9	0.67	0.69	0.67	0.72	0.66	0.65
Pb	2.4	2.6	3.1	2.8	2.6	2.4	14	14	14	13	13	13
Th	3.5	5.5	6.4	6.9	6.6	6.6	5.9	6.0	5.9	6.1	5.8	5.9
U	0.71	1.5	1.7	1.8	1.8	1.5	1.2	1.2	1.3	1.3	1.2	1.2
PGE (ppb)												
Ir	0.017	0.018	0.028	0.008	0.009	0.007	0.006	0.006	0.006	0.010	0.006	0.006
Ru	0.026	0.015	0.012	0.011	0.017	0.012	0.011	0.014	0.018	0.025	0.015	0.012
Rh	0.018	0.003	0.003	0.004	0.003	0.003	0.005	0.004	0.016	0.014	0.006	0.007
Pt	0.164	0.015	0.135	0.035	0.039	0.080	0.034	0.047	0.094	0.063	0.053	0.027
Pd	0.501	0.240	0.361	0.272	0.472	1.370	0.072	0.221	0.089	0.098	0.243	0.095
Elemental ratios												
Cu/Pd	122,000	168,000	100,000	117,000	76,000	22,000	257,000	63,000	142,000	112,000	45,000	150,000
Pd/Ir	30	13	13	33	50	184	13	40	16	10	40	17
Pt/Rh	9.1	5.1	42.7	10.0	14.6	28.1	7.1	12.5	5.7	4.6	9.6	4.1

5.2. Chalcophile elements

5.2.1. Leiqiong basaltic rocks

Most of the Leiqiong mafic rocks have low chalcophile element abundances, but one Mg-rich sample, HWGA, is highly enriched in both PGE and Ni. The compositional ranges are 66–316 ppm Ni, 30–73 ppm Cu, 0.004–0.224 ppb Ir, and 0.114–1.797 ppb Pd (Table 1 and Appendix 2). The rocks have high Cu/Pd ratios (22,671 to 474,768) with moderate Pd/Ir and Pt/Rh ratios (6.1–58 and 1.07–14, respectively). They all display similar U-shaped patterns with depleted PGE relative to Cu and Ni in primitive mantle-normalized PGE diagrams and exhibit generally increasing trends from Ir to Pd (Fig. 5a). All but the Mg-rich sample, HWGA, plot in the MORB field (Fig. 5a). Most of the samples show a moderate depletion in Pt, leading to flat patterns between Rh to Pt.

5.2.2. Sanshui basaltic rocks

The Sanshui lavas have generally lower chalcophile element contents than the mafic rocks of Leiqiong, with 45–58 ppm Ni, 30–

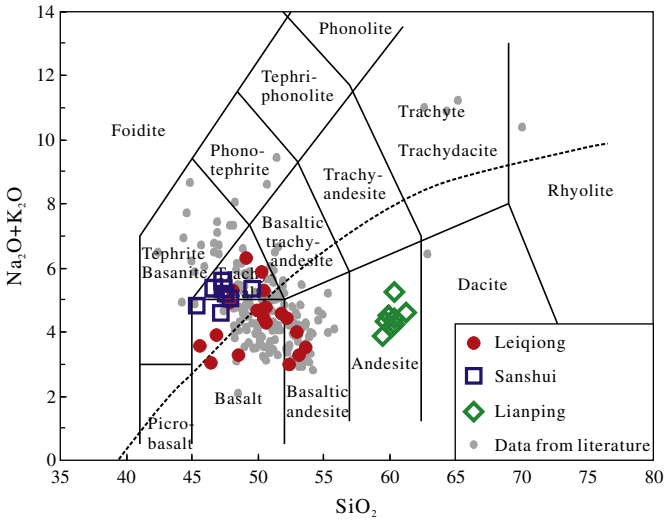

Fig. 3. TAS diagram for volcanic rocks from Leiqiong, Sanshui and Lianping, SE China, after Le Maitre (1989). Data for the Leiqiong basalts are from Han et al. (2009). Previous data of volcanic rocks from SE China (gray dots) are from Zhou and Armstrong (1982); Fan and Hooper (1991); Liu et al. (1995); Chung et al. (1997), Chung (1999); Ho et al. (2000); Xie et al. (2001).

40 ppm Cu, 0.006–0.028 ppb Ir and 0.22–1.69 ppm Pd. They have higher Pt/Rh (5.14–43) and Pd/Ir ratios (13–185) and lower Cu/Pd ratios (19,600–167,700) relative to samples from Leiqiong and Lianping. The primitive mantle-normalized PGE plots of these samples show U-shaped patterns with slightly negative Ru anomalies (Fig. 5b).

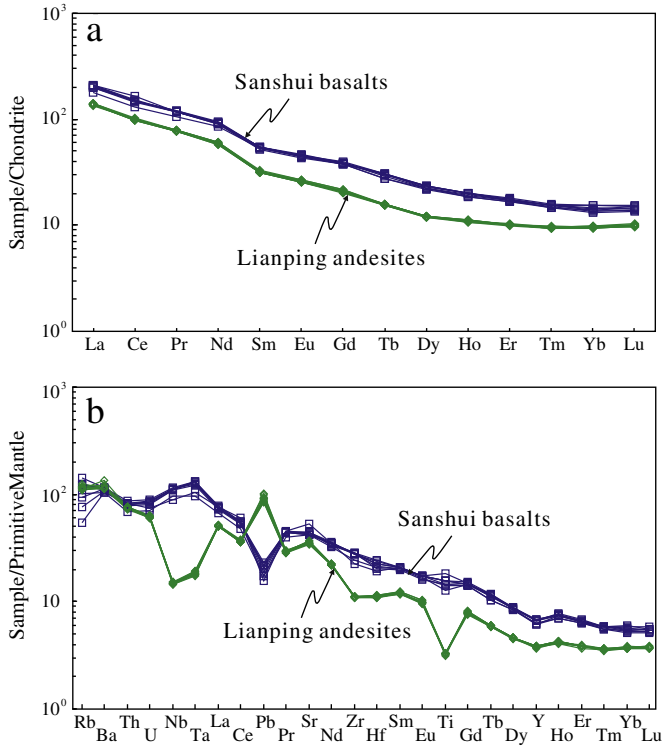

Fig. 4. a. REE patterns for volcanic rocks from Sanshui and Lianping, SE China. Chondrite data are from Sun and McDonough (1989). b. Spider diagrams for volcanic rocks from Sanshui and Lianping, SE China. Primitive mantle data are from McDonough and Sun (1995).

5.2.3. Lianping andesites

The Lianping andesites are lower in chalcophile element than the mafic rocks from Sanshui and Leiqiong, with 16–19 ppm Ni and 11–19 ppm Cu (Table 1). They also show lower Pt/Rh (4.13–14) and Pd/Ir ratios (10–40) and higher Cu/Pd ratios (45,000–184,000) than the mafic rocks. The primitive mantle-normalized PGE plots of these samples show U-shaped patterns (Fig. 5c). Both the Sanshui and Lianping volcanics have limited major and trace element compositions (Figs. 3 and 4, Table 1 and Appendix 2) and slightly varying PGE patterns.

6. Discussion

6.1. Controls on the PGE distributions

Volcanic rocks in SE China show large variations in PGE contents (Table 1 and Appendix 2), which are thought to reflect both crystal fractionation and sulfide segregation. Olivine and chromite may fractionate IPGE from PPGE, because these two minerals have different partition coefficients for these element groups (Barnes et al., 1985; Brügmann et al., 1987). Crystallization of alloys or discrete metal clusters would deplete some particular PGEs (Merkle, 1992; Peck and Keays, 1990a; Tredoux et al., 1995), whereas segregation of sulfides (Barnes and Picard, 1993; Campbell and Naldrett, 1979; Maier et al., 1996) depletes all PGEs in magmas.

6.1.1. Olivine fractionation

Mafic rocks in Leiqiong show positive correlations of MgO with Ni and Cr (Fig. 6a and b), indicating fractionation of olivine and chromite. Such fractionation is supported by the appearance of olivine phenocrysts with chromite inclusions in some of the Leiqiong samples (Fig. 2c and d).

Olivine-rich sample HWGA has the highest MgO (>10 wt.%) and PGE contents with a high IPGE/PPGE ratio (Fig. 5a). Abundant olivine xenocrysts and phenocrysts in the sample explain the relatively high PGE (particularly IPGE) concentrations. However, the large PGE variation of the Sanshui and Lianping samples at constant MgO and the lack of obvious correlations between PGEs and MgO (Fig. 7) suggests that olivine fractionation may not be the main control on the PGE concentrations.

6.1.2. Chromite fractionation

Rocks from Lianping and Leiqiong show positive correlations between Ir and Ru (Fig. 8), suggesting that the partition coefficients of Ir and Ru between the different phases in these rocks are similar during magmatic evolution. However, volcanic rocks from Sanshui do not show similar positive correlation between Ru and Ir, and several samples exhibit depletion of Ru relative to Ir (Fig. 5b), indicating removal of one or more phases that host more Ru than Ir or presence of discrete Ir-rich microphases such as Ir-rich alloy.

Crystallization of chromite during an early stage of fractionation may cause the depletion of Ru, because Ru is compatible in chromite (e.g., Capobianco and Drake, 1990; Locmelis et al., 2011; Merkle, 1992; Righter et al., 2004). Negative Ru anomalies of basalts and positive Ru anomalies of ultramafic rocks and chromites elsewhere in the world all suggest a close relationship between Ru and chromite (Angeli et al., 2001; Aulbach et al., 2004; Büchl et al., 2004; Chazey and Neal, 2005; Fiorentini et al., 2004; Handler and Bennett, 1999; Lorand et al., 2004; Philipp et al., 2001; Zhou et al., 1998). On the other hand, olivine crystals in some Sanshui samples with Ir enrichment have high Fo numbers (up to 85), suggesting relatively early crystallization of olivine. Ir-rich alloy grains can be trapped very early within olivine grains to avoid interaction with evolved magmas that fall below PGM saturation after sulfide fractionation (Barnes and Fiorentini, 2008). Therefore, we infer that the Ru depletion relative to Ir of some samples from Sanshui (Fig. 5b) indicates fractionation of

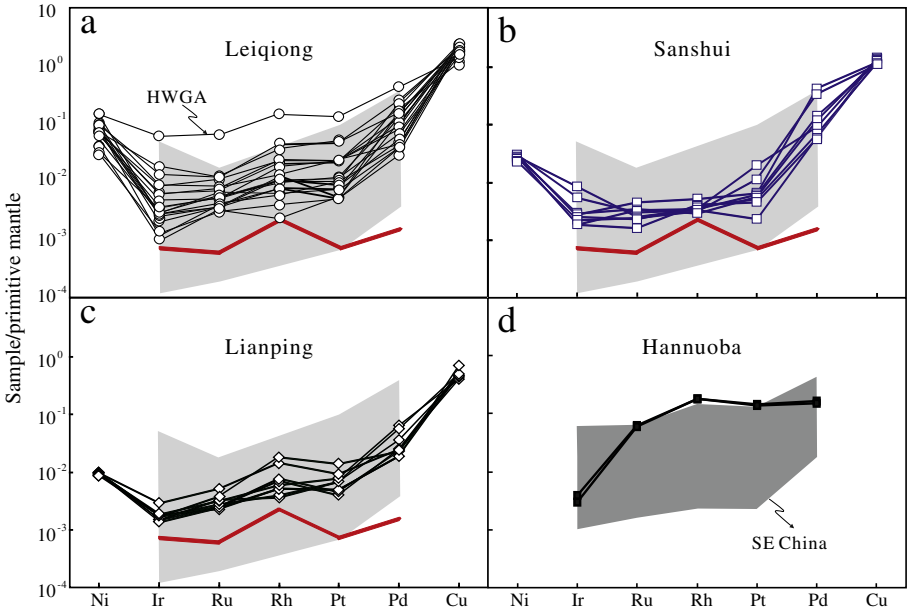

Fig. 5. Primitive mantle-normalized PGE patterns for volcanic rocks from a) Leiqiong, b) Sanshui, c) Lianping, and d) Hannuoba. Data of the Hannuoba basalts are from Chu et al. (1999). Primitive mantle data are from Taylor and McLennan (1985). The line at the bottom of each diagram indicates the detection limits for PGEs. The shaded area in a, b and c shows the range of PGE in MORB based on data from Devey et al. (1994); Rehkämper et al. (1999); Tatsumi et al. (1999); Bézos et al. (2005). The shaded area in d shows the PGE patterns for volcanic rocks of SE China from this study.

chromite from the primary magma and/or accumulation of olivine with Ir-alloys.

6.1.3. Sulfide fractionation

The depletion of PGE relative to Ni and Cu (Fig. 5) suggests that the magmas were S-saturated before their eruption, because sulfide removal would deplete PGE more than Ni and Cu. Sulfide segregation may have taken place in the mantle source and/or during the evolution of the magmas.

Cu, Zr and Pd behave as incompatible elements in S-undersaturated magmas resulting in mantle-like Cu/Pd ratios and constant Cu/Zr ratios

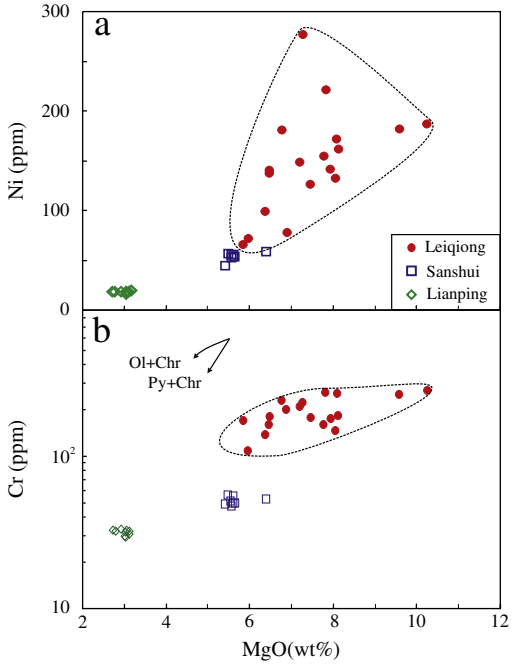

Fig. 6. a and b. Plots of Ni and Cr vs. MgO for volcanic rocks from Leiqiong, Sanshui and Lianping, SE China. The fractionation trends of Ol + Chr and Py + Chr are from Song et al. (2009). Abbreviations: Py — pyroxene; Sul — sulfide.

of mafic rocks (e.g., Cu/Zr 1–3 in the Noril'sk basalt; Naldrett, 2004). On the other hand, removal of sulfide in S-saturated magmas would result in Cu/Zr ratios lower than 1 (Lightfoot et al., 1994) and Cu/Pd ratios higher than mantle values (~7000, Barnes and Maier, 1999). All samples from SE China have Cu/Zr ratios less than 1 (Fig. 9a and b) and very high and variable Cu/Pd ratios (Fig. 9c, and Table 1), indicating removal of sulfides during magmatic evolution. Cu decreases with decreasing Cu/Zr ratios, whereas Zr exhibits an opposite trend (Fig. 9a and b), which is consistent with S-saturated fractionation. This scenario is consistent with the observed positive correlations between Ni and Cu (Fig. 9d), which have comparable partition coefficients between sulfide liquid and silicate magma (Barnes and Lightfoot, 2005).

Cu/Pd ratios of samples from Lianping and Sanshui show large variations with a small range of Cu contents (Fig. 9c), indicating a process which exerts considerable influence on Pd contents but much less on Cu concentrations. Considering that the only host of Pd is sulfide and that the partition coefficient of Pd between sulfide liquid and silicate melt is much higher than that of Cu, the variations are most likely due to segregation of a small amount of immiscible sulfides.

Pd/Cr ratios increase with decreasing Ni/Pd during fractionation under S-undersaturated conditions, whereas Pd/Cr ratios dramatically decrease with increasing Ni/Pd ratios in S-saturated magmas (Song et al., 2006). Therefore, the negative correlation between Ni/Pd and Pd/Cr ratios also indicates sulfide segregation during magmatic evolution in the three volcanic suites (Fig. 10).

6.1.4. Quantitative modeling of immiscible sulfide removal

The geochemical data presented above indicate that the volcanic rocks from Leiqiong, Sanshui and Lianping have undergone sulfide-saturated fractionation. Because Cu and Pd are both incompatible elements in sulfide-undersaturated magmas and Pd has a much larger partition coefficients into sulfides, the depletion of Pd relative to Cu (expressed as the increase in Cu/Pd ratios) is purely caused by segregation of sulfides. Consequently, we could use Cu/Pd vs. Pd diagrams to model the mass fractions of early removed sulfides. In modeling, we adopt the sulfide/silicate melt partition coefficients of 1000 for Cu and 35,000 for Pd (Francis, 1990; Peach et al., 1990) and presume them to remain constant during sulfide segregation. We chose the points where the extrapolated trend lines of the samples intersect

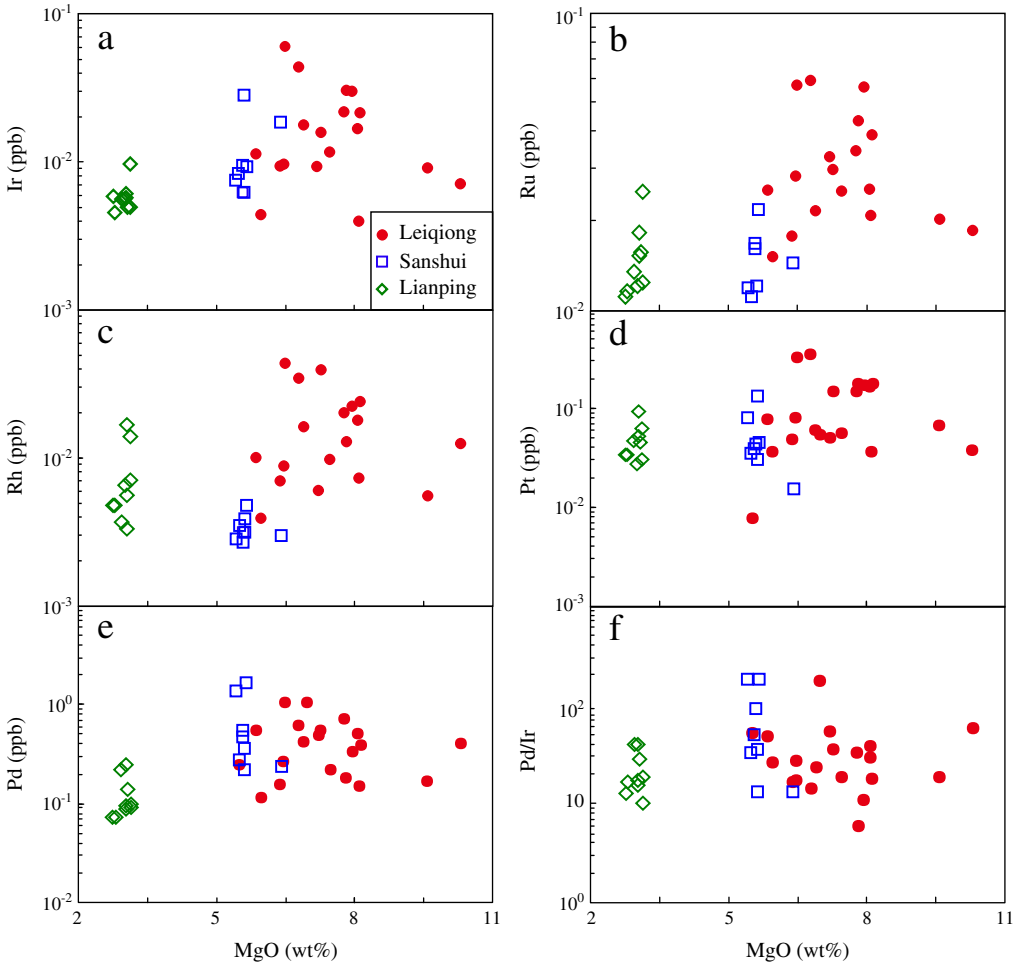

Fig. 7. Plots of Ir, Ru, Rh, Pt, Pd and Pd/Ir vs. MgO for volcanic rocks from Leiqiong, Sanshui and Lianping, SE China.

with the primitive mantle Cu/Pd line to represent the initial compositions of the magmas (Fig. 11). The modeled curves indicate that the Leiqiong, Sanshui and Lianping magmas were all depleted in sulfides relative to primitive magma with mantle-like Cu/Pd ratios (Fig. 11). Assuming no sulfides retained in the source, 0.013%, 0.009% and 0.01% mass fractions of sulfides segregated from the primitive Leiqiong, Sanshui and Lianping magmas, respectively. Considering that sulfides might be retained in the source during partial melting, the actual segregated amount during magmatic evolution would be smaller than the modeled results. Thus, the amount of segregated sulfides from volcanic rocks in SE China is lower compared to that from MORB (0.012–0.084%, Bézos et al., 2005)

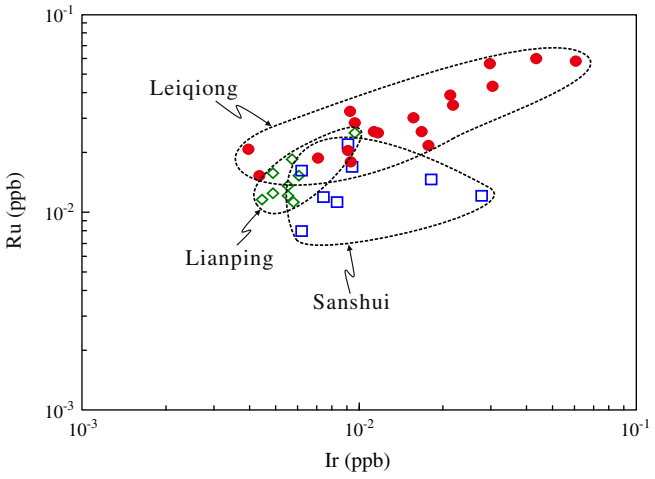

Fig. 8. Ru vs. Ir plots for volcanic rocks from Leiqiong, Sanshui and Lianping, SE China. Fields encompass the data for the three magmatic suites.

6.2. Nature of mantle sources

Some samples from SE China show Pt depletion relative to Rh and Pd with Pt/Rh ratios ranging from 1.07 to 43 (Table 1 and Appendix 2). In particular, rocks from Lianping and Leiqiong have low Pt/Rh ratios with strong Pt depletion. A possible explanation for the Pt depletion is that the magmas underwent fractionation of Fe–Pt alloys during an early stage of crystallization of chromite (Bai et al., 2000; Cabri, 1992; Nixon and Hammack, 1991; Peck and Keays, 1990a, b). The early separation of Fe–Pt alloys included in chromites could possibly account for the Pt-depletion in some of Sanshui samples due to the concurrent depletion of Ru. However, linear correlations of Pt with Ir and Ru of samples from Lianping and Leiqiong (Fig. 12) indicate that Pt may not be depleted during magmatic evolution. Some other mechanism is required to deplete the magmas in Pt and thus the Pt-depleted signature was probably inherited from their mantle sources.

Depletion of Pt in mantle peridotites implies a unique mode of mobility of Pt during melt-rock interaction relative to other PGEs. It is thought to be due to selective Pt loss from sulfides via the exsolution of Pt–Te–Bi-rich phases from primary sulfides during serpentinization and interaction with melts (Ackerman et al., 2009; Alard et al., 2000; Luguet et al., 2004). Thus, possibly partial melting of such a mantle source, from which Pt-rich phases may have been removed,

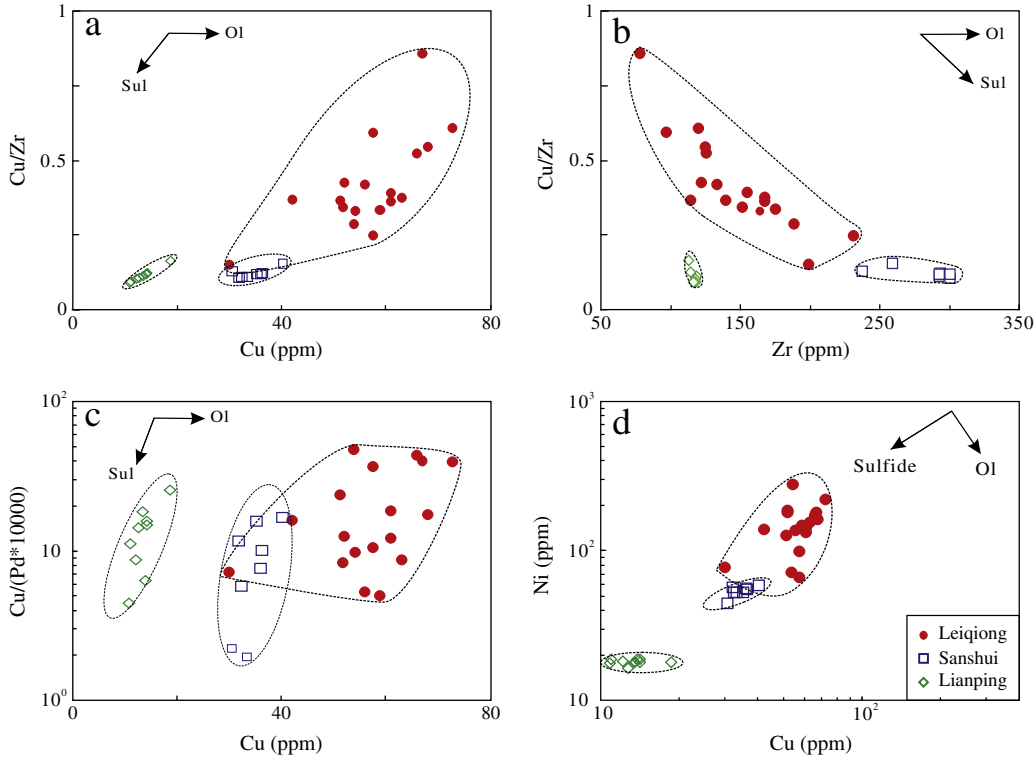

Fig. 9. Plots of Cu and Zr vs. Cu/Zr and Cu/Pd and Ni vs. Cu for volcanic rocks from Leiqiong, Sanshui and Lianping, SE China.

generated the volcanic rocks in Lianping and Leiqiong with varying degrees of Pt depletion.

If some sulfides remain in the mantle during partial melting, high Pd/Ir ratios of the magma are often attributed to relatively "dry" melting conditions. Under "dry" conditions, Os–Ir–Ru–Rh-enriched Mss behaves in a refractory manner, resulting in super-chondritic Pd/Ir ratios in the magma. Under fluid-rich melting conditions, alloys and Mss are more fusible, resulting in PGE ratios closer to chondrite (Maier and Barnes, 2004). The Pd/Ir ratios are very low in the Lianping andesites (10.1–40.0) and Leiqiong basalts (6.1–58) but relatively high in the Sanshui basalts (13.0–184.5). This suggests that the Sanshui magmas with high Pd/Ir ratios may have formed under "dry" melting conditions, whereas the Lianping and Leiqiong mantle sources underwent stronger melt/fluid metasomatism.

The negative Nb–Ta and Zr–Hf anomalies of andesites in Lianping may reflect a depleted nature of the mantle source which was affected by subduction-related fluids. Isotopic studies on basalts from Leiqiong suggest an EMII component in their source, which is believed to be pyroxenite formed by melt-metasomatism of the lithospheric mantle (e.g. Han et al., 2009; Xu., 1999). Such fluid/melt metasomatism in the lithospheric mantle below SE China is also documented in mantle xenoliths (e.g. Fan and Menzies, 1992; Tatsumoto et al., 1992; Xu et al., 2003; Yu et al., 2006). Possible metasomatic media include fluids/melts associated with the subduction of the Paleo-Pacific Plate (Tatsumoto et al., 1992), and/or melts related

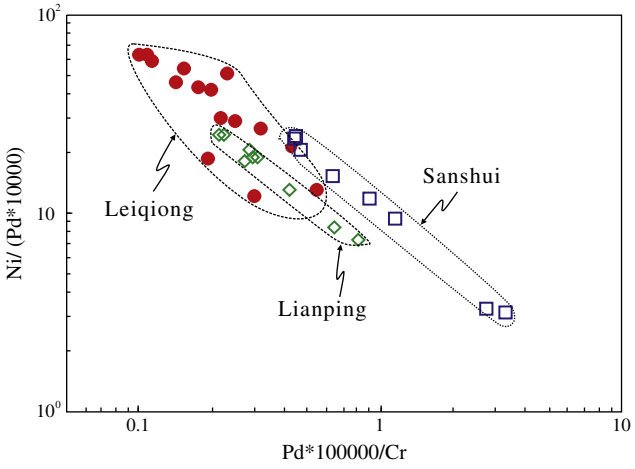

Fig. 10. Plots of Ni/(Pd*10,000) vs. Pd*100,000/Cr for volcanic rocks from Leiqiong, Sanshui and Lianping, SE China.

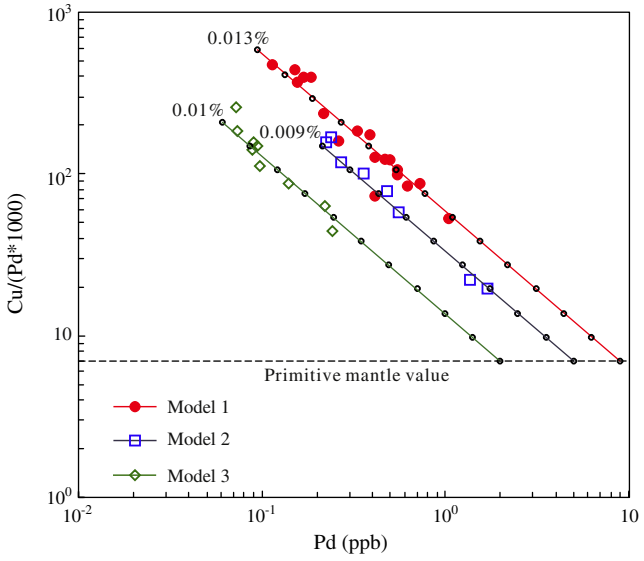

Fig. 11. Cu/(Pd*10,000) vs. Pd plots for volcanic rocks from Leiqiong, Sanshui and Lianping, SE China. Models 1, 2 and 3 (for Leiqiong, Sanshui and Lianping, respectively) show the trends of silicate magmas, starting with 8.9 ppb Pd and 62.3 ppm Cu, 5 ppb Pd and 35 ppm Cu and 2 ppb Pd and 14 ppm Cu. Small circles on the curves correspond to intervals representing 0.001% sulfide segregation of the original liquid. See text for details.

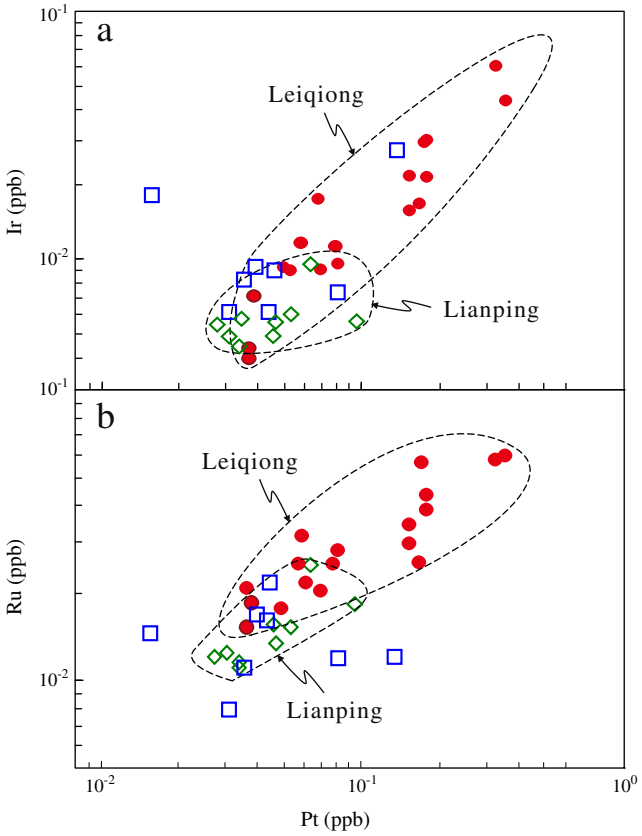

Fig. 12. Ir, Ru and Rh vs. Pt plots for volcanic rocks from Leiqiong, Sanshui and Lianping, SE China.

to the opening and post-spreading of the South China Sea (Yu et al., 2006).

6.3. Implications for the genesis of eastern China basalts

The Cenozoic volcanic rocks in SE and NE China show different isotopic compositions due to varied SCLM compositions beneath the two regions (e.g., Zou et al., 2000). SE China is underlain by relatively young, middle to late Proterozoic continental lithosphere, whereas NE China is underlain by Archaean to early Proterozoic continental lithosphere (e.g., Chen and Jahn, 1998). PGE geochemistry of volcanic rocks in SE China, with significantly lower PGE concentrations, is also distinctly different from that of the Hannuoba basalts, NE China (Chu et al., 1999). Sample HWGA has PGE contents comparable with those of the Hannuoba basalts but shows no strong Ir-depletion (Fig. 5). The PGE differences may also reflect varied source natures.

Due to the high metal/silicate distribution coefficient of Ir at low fO_2 conditions, strong depletion of Ir relative to other PGEs in basalts and mantle xenoliths of NE China is commonly attributed to the retention of an Ir-rich phase in the deep mantle during partial melting (Amossé et al., 1990; Chu et al., 1999; Orberger et al., 1998; Xu et al., 1998). Previous studies show that the redox state of the SCLM beneath SE China is similar to that of peridotite xenoliths from other continental regions (Qi et al., 1995) and higher than that of NE China (Li and Wang, 2002; Xu, 1994). Therefore, the more oxidized SCLM beneath SE China may have prevented Ir retention in the deep mantle, which can account for the absence of strong Ir-depletion in the volcanic rocks in SE China.

The PGE concentrations of volcanic rocks from NE China are much higher than those from SE China, which may be explained by two factors. First, most mantle xenoliths discovered in NE China have relatively low S contents near or less than 100 ppm (Reisberg et al., 2005; Zheng et al., 2005). Therefore, moderate degrees (~10%) of partial melting would exhaust all the sulfides in the mantle and produce magmas with high PGE concentrations. Second, experimental and empirical studies (see review by Carrol and Webster, 1994; Naldrett, 2004) have shown that the solubility of sulfide at sulfide saturation in mafic magmas increases with decreasing fO_2. Therefore, under relatively low redox state in the SCLM under NE China, magma may have not reached sulfide saturation during its evolution, preventing depletion of PGEs by segregation of immiscible sulfides.

From Mesozoic to Cenozoic, the SCLM beneath SE China has continuously suffered from metasomatism associated with the subduction of the Paleo-Pacific Plate and magmatism during the spreading and post-spreading of the South China Sea and became heterogeneous. In the early Paleogene, eastern China has experienced extension due to the Indo-Asian collision and/or the rollback of the subducting Paleo-Pacific Plate, leading to thinning of the lithosphere, upwelling of the asthenospheric mantle and widespread Cenozoic volcanism (Liu et al., 2004; Northrup et al., 1995). Upwelling of the asthenospheric mantle in NE China incorporated the ancient EM1 component in the SCLM and generated Ir-depleted basalts, such as those in Hannuoba, whereas asthenospheric upwelling under SE China incorporated the heterogeneously metasomatized SCLM and produced basalts with MORB-like PGE patterns such as the Leiqiong basalts.

However, there is a lack of complete chalcophile element data for basalts from NE China in the literature. Further studies on PGEs in basalts of NE China are needed to clarify the differences between the volcanic rocks from NE and SE China.

7. Conclusions

Cenozoic basalts and andesites in SE China do not display strong Ir-depletion that is common in basalts and associated mantle xenoliths in NE China. The lack of strong Ir depletion in the volcanic rocks of SE China is attributed to increased solubility of Ir in silicate phases under higher fO_2 conditions, implying more oxidized SCLM beneath SE China than NE China. The generally lower total PGE in the volcanic rocks of SE China resulted from sulfide retention in the source and/or S-saturated crystal fractionation.

Basalts at Leiqiong evolved by fractionating olivine and chromite, whereas those at Sanshui fractionated olivine, chromite and an Fe–Pt alloy. Volcanic rocks from SE China underwent sulfide segregation during magmatic evolution, but the amount of segregated sulfides was small compared to that in the case of MORB.

Depletion of Pt relative to other PGEs in volcanic rocks from Leiqiong and Lianping most likely reflects derivation from a Pt-depleted mantle source. Pt depletion in the mantle source was due to fluid/melt-metasomatism of the SCLM.

Acknowledgments

This study was funded by the Key Laboratory of Marine Hydrocarbon Resources and Environmental Geology, Ministry of Land and Resources (MRE200908), the China Ocean Mineral Resources R&D Association (DYXM-115-02-3-03) and the Natural Science Foundation of China (No. 40873020). The authors are grateful to Prof. Xiaolin Xiong and Zhaoyu Zhu and Dr. Jiangwei Han for providing the Leiqiong samples, to Ying Liu and Guangqian Hu for help with major and trace element analysis. The manuscript benefited greatly from discussions with Jianfeng Gao and Wei Terry Chen. We thank Prof. Eero Hanski and an anonymous reviewer for careful and constructive reviews and editor in-chief Dr Andrew Kerr for the helpful comments and suggestions. This is contribution No. IS-1384 from GIGCAS.

Appendix 1. Analytical results of PGE for reference materials WGB-1 (gabbro) and TDB-1 (diabase).

Elements	WGB-1 (gabbro)			TDB-1 (diabase)		
	Average (n = 5)	Meisel	Certified	Average (n = 5)	Meisel	Certified
Ir (ppb)	0.17 ± 0.02	0.211	0.33	0.083 ± 0.011	0.075	0.15
Ru (ppb)	0.13 ± 0.01	0.144	0.30	0.21 ± 0.02	0.198	0.30
Rh (ppb)	0.22 ± 0.02	0.234	0.32	0.49 ± 0.03	0.471	0.70
Pt (ppb)	6.29 ± 0.68	6.39	6.10	5.18 ± 0.28	5.01	5.80
Pd (ppb)	13.2 ± 1.01	13.9	13.9	23.4 ± 1.2	24.3	22.4

Meisel = (Meisel and Moser, 2004). Certified = (Govindaraju, 1994).

Appendix 2. Major and trace elements and PGE concentrations of additional samples from SE China.

Locality	Leiqiong						Sanshui			Lianping		
Sample	HLMA	GD9	18	GD137	SY10	CK280	SS-24	SS-26	SS-30	LP-4	LP-5	LP-6
Rock type	b. andesite	b. andesite	basalt	basalt	t. basalt	basalt	basalt	basalt	basalt	andesite	andesite	andesite
Oxides (wt.%)												
SiO_2	53	52	46	46	51	52	47	48	47	61	60	60
TiO_2	1.7	1.6	1.6	1.9	1.9	1.6	2.6	2.7	2.7	0.67	0.68	0.68
Al_2O_3	14	14	14	14	17	15	17	17	17	17	17	17
Fe_2O_3	11	10	10	10	10	10	10	11	11	5	6	6
MnO	0.14	0.14	0.14	0.15	0.13	0.12	0.16	0.16	0.16	0.10	0.11	0.11
MgO	6.4	9.6	10.3	8.1	6.0	7.2	5.6	5.6	5.6	2.8	3.1	3.1
CaO	9.0	8.9	8.0	10.0	8.8	6.8	8.5	9.2	8.9	6.0	6.1	6.0
Na_2O	3.1	2.8	2.8	2.8	3.9	3.4	3.8	4.0	4.0	3.2	2.6	2.8
K_2O	0.22	0.21	0.20	0.79	1.5	1.2	1.5	1.3	1.2	2.2	2.0	2.1
P_2O_5	0.19	0.14	0.24	0.25	0.34	0.23	0.91	0.93	0.94	0.40	0.41	0.42
L.O.I	1.3	0.46	6.4	6.6	0.36	3.2	3.3	2.8	2.3	1.5	1.8	1.7
Total	100	100	100	100	101	100	100	103	100	100	100	100
Mg#	56	69	70	65	58	63	56	54	55	55	57	56
Trace elements (ppm)												
Sc	19	19	20	22	18	14	18	18	18	11	11	11
V	135	136	138	172	144	115	186	183	191	94	95	98
Cr	146	270	291	275	114	225	51	49	51	33	32	33
Ni	99	182	187	172	71	149	53	53	53	18	19	18
Cu	58	67	52	66	54	59	33	32	35	13	14	12
Rb	7	12	22	22	26	23	46	74	56	71	68	66
Sr	257	267	397	594	587	474	872	849	871	713	715	703
Y	13	13	12	15	13	14	27	26	27	16	16	17
Zr	97	78	122	126	189	176	298	293	293	119	115	118
Nb	11	7	26	27	5	26	73	73	73	10	10	10
Ba	109	113	249	249	364	250	713	722	750	798	893	767
La	6	6	15	16	18	16	47	48	49	34	33	32
Ce	12	13	29	32	35	33	90	91	92	62	62	61
Pr	1.8	1.8	3.5	3.8	4.2	4.0	11.1	11.3	11.6	7.6	7.6	7.5
Nd	8	8	14	16	16	16	42	43	45	28	28	28
Sm	2.6	2.5	3.3	3.8	3.9	3.8	8.1	8.2	8.5	5.0	5.0	4.9
Eu	1.2	1.0	1.3	1.3	1.6	1.4	2.5	2.6	2.7	1.6	1.6	1.5
Gd	3.0	2.8	3.3	3.7	3.8	3.6	7.8	7.8	8.1	4.4	4.5	4.3
Tb	0.49	0.45	0.51	0.56	0.56	0.55	1.03	1.03	1.10	0.59	0.60	0.60
Dy	2.7	2.6	2.8	3.1	3.0	2.8	5.6	5.7	5.8	3.1	3.1	3.1
Ho	0.48	0.50	0.48	0.54	0.51	0.49	1.04	1.06	1.11	0.63	0.63	0.63
Er	1.2	1.3	1.2	1.4	1.2	1.2	2.8	2.7	2.8	1.7	1.7	1.7
Tm	0.17	0.17	0.17	0.20	0.17	0.16	0.39	0.38	0.40	0.24	0.25	0.25
Yb	1.0	1.0	1.0	1.2	1.0	1.0	2.3	2.3	2.4	1.6	1.7	1.6
Lu	0.14	0.15	0.15	0.18	0.16	0.15	0.36	0.34	0.37	0.25	0.26	0.26
Hf	2.4	2.1	2.9	2.8	4.3	3.6	5.8	6.0	6.3	3.3	3.3	3.2
Ta	0.57	0.5	1.7	1.7	0.2	1.5	4.6	4.7	4.8	0.71	0.66	0.66
Pb	0.93	2.3	1.5	1.0	1.9	1.6	3.2	3.5	3.3	15	15	13
Th	0.93	1.4	2.4	2.2	3.1	2.4	6.2	6.6	6.5	6.1	6.0	6.1
U	0.20	0.30	0.64	0.57	0.71	0.61	1.7	1.7	1.7	1.2	1.3	1.2
PGE (ppb)												
Ir	0.009	0.009	0.007	0.004	0.004	0.009	0.009	0.006	0.006	0.004	0.005	0.005
Ru	0.018	0.020	0.019	0.021	0.015	0.033	0.022	0.016	0.008	0.012	0.012	0.016
Rh	0.007	0.006	0.013	0.007	0.004	0.006	0.005	0.003	0.004	0.005	0.007	0.003
Pt	0.049	0.068	0.038	0.036	0.036	0.051	0.045	0.043	0.031	0.034	0.030	0.045
Pd	0.156	0.168	0.412	0.150	0.114	0.482	1.694	0.560	0.223	0.073	0.090	0.139
Elemental ratios												
Cu/Pd	368,000	399,000	126,000	438,000	475,000	50,000	20,000	58,000	157,000	184,000	157,000	87,000
Pd/Ir	17	18	58	38	26	54	185	90	36	16	18	28
Pt/Rh	7.0	12.4	3.0	4.9	9.3	8.5	9.5	13.6	8.0	7.1	4.3	13.7

References

Ackerman, L., Walker, R.J., Puchtel, I.S., Pitcher, L., Jelinek, E., Strnad, L., 2009. Effects of melt percolation on highly siderophile elements and Os isotopes in subcontinental lithospheric mantle: a study of the upper mantle profile beneath Central Europe. Geochimica et Cosmochimica Acta 73, 2400–2414.

Alard, O., Griffin, W.L., Lorand, J.P., Jackson, S.E., O'Reilly, S.Y., 2000. Non-chondritic distribution of the highly siderophile elements in mantle sulphides. Nature 407, 891–894.

Amossé, J., Allibert, M., Fischer, W., Piboule, M., 1990. Experimental study of the solubility of platinum and iridium in basic silicate melts: implications for the differentiation of platinum-group elements during magmatic processes. Chemical Geology 81, 45–53.

Angeli, N., Fleet, M.E., Thibault, Y., Candia, M.A.F., 2001. Metamorphism and PGE-Au content of chromitite from the Ipanema mafic/ultramafic Complex, Minas Gerais, Brazil. Mineralogy and Petrology 71, 173–194.

Aulbach, S., Griffin, W.L., Pearson, N.J., O'Reilly, S.Y., Kivi, K., Doyle, B.J., 2004. Mantle formation and evolution, Slave Craton: constraints from HSE abundances and Re–Os isotope systematics of sulfide inclusions in mantle xenocrysts. Chemical Geology 208, 61–88.

Bai, W.J., Robinson, P.T., Fang, Q.S., Yang, J.S., Yan, B.G., Zhang, Z.M., Hu, X.F., Zhou, M.F., Malpas, J., 2000. The PGE and base-metal alloys in the podiform chromitites of the Luobusa ophiolite, southern Tibet. The Canadian Mineralogist 38, 585–598.

Barnes, S.J., Fiorentini, M.L., 2008. Iridium, ruthenium and rhodium in komatiites: evidence for iridium alloy saturation. Chemical Geology 257, 44–58.

Barnes, S.-J., Lightfoot, P.C., 2005. Formation of magmatic nickel sulfide ore deposits and processes affecting their copper and platinum group element contents: Economic Geology 100th Anniversary, Volume 34, pp. 179–214.

Barnes, S.-J., Maier, W., 1999. The fractionation of Ni, Cu and the noble metals in silicate and sulfide liquids. In: Keays, R.R. (Ed.), Dynamic processes in magmatic ore deposits and their application to mineral exploration: Geological Association of Canada, Short Course Notes, 13, pp. 69–106.

Barnes, S.-J., Picard, C.P., 1993. The behaviour of platinum-group elements during partial melting, crystal fractionation, and sulphide segregation: an example from the Cape Smith Fold Belt, northern Quebec. Geochimica et Cosmochimica Acta 57, 79–87.

Barnes, S.-J., Naldrett, A.J., Gorton, M.P., 1985. The origin of the fractionation of platinum-group elements in terrestrial magmas. Chemical Geology 53, 303–323.

Bézos, A., Lorand, J.P., Humler, E., Gros, M., 2005. Platinum-group element systematics in Mid-Oceanic Ridge basaltic glasses from the Pacific, Atlantic, and Indian Oceans. Geochimica et Cosmochimica Acta 69, 2613–2627.

Brügmann, G.E., Arndt, N.T., Hofmann, A.W., Tobschall, H.J., 1987. Noble metal abundances in Komatiite suites from Alexo, Ontario, and Gorgona Island, Colombia. Geochimica et Cosmochimica Acta 51, 2159–2169.

Büchl, A., Brugmann, G., Batanova, V.G., 2004. Formation of podiform chromitite deposits: implications from PGE abundances and Os isotopic compositions of chromites from the Troodos complex, Cyprus. Chemical Geology 208, 217–232.

Cabri, L.J., 1992. The distribution of trace precious metals in minerals and mineral products. Mineralogical Magazine 56, 289–308.

Campbell, I., Naldrett, A., 1979. The influence of silicate/sulfide ratios on the geochemistry of magmatic sulfides. Economic Geology 74, 1503.

Capobianco, C.J., Drake, M.J., 1990. Partitioning of ruthenium, rhodium, and palladium between spinel and silicate melt and implications for platinum group element fractionation trends. Geochimica et Cosmochimica Acta 54, 869–874.

Carrol, M., Webster, S., 1994. Solubilities of sulphur, noble gases, nitrogen, chlorine and fluorine. Reviews in Mineralogy 30, 231.

Chazey, W.J., Neal, C.R., 2005. Platinum-group element constraints on source composition and magma evolution of the Kerguelen Plateau using basalts from ODP Leg 183. Geochimica et Cosmochimica Acta 69, 4685–4701.

Chen, J., Jahn, B., 1998. Crustal evolution of southeastern China: Nd and Sr isotopic evidence. Tectonophysics 284, 101–133.

Chu, X.L., Li, X.L., Xu, J.H., Liu, J.M., 1999. Patterns of platinum-group elements in mantle peridotite, granulite xenoliths and basalt in Hannuoba. Chinese Science Bulletin 44, 1676–1681 (in Chinese).

Chung, S.L., 1999. Trace element and isotope characteristics of Cenozoic basalts around the Tanlu fault with implications for the eastern plate boundary between North and South China. Journal of Geology 107, 301–312.

Chung, S.L., Sun, S.S., Tu, K., Chen, C.H., Lee, C.Y., 1994. Late Cenozoic basaltic volcanism around the Taiwan Strait, SE China: product of lithosphere–asthenosphere interaction during continental extension. Chemical Geology 112, 1–20.

Chung, S.L., Cheng, H., Jahn, B.M., Oreilly, S.Y., Zhu, B.Q., 1997. Major and trace element, and Sr–Nd isotope constraints on the origin of Paleogene volcanism in South China prior to the South China sea opening. Lithos 40, 203–220.

Cong, B.L., Zhang, W.H., Ye, D.N., 1979. The study on the Cenozoic basalts in North China fault block. Acta Geologica Sinica 2, 112–124 (in Chinese with English abstract).

Devey, C., Garbe-Schönberg, C.D., Stoffers, P., Chauvel, C., Mertz, D., 1994. Geochemical effects of dynamic melting beneath ridges: reconciling major and trace element variations in Kolbeinsey (and global) mid-ocean ridge basalt. Journal of Geophysical Research 99, 9077–9095.

Fan, Q.C., Hooper, P.R., 1991. The Cenozoic basaltic rocks of eastern China: petrology and chemical composition. Journal of Petrology 32, 765–810.

Fan, W.M., Menzies, M.A., 1992. The composition of lithospheric mantle in rifting volcanism environment: geochemical evidence from Cenozoic basaltic rocks from Leiqiong area. In: Liu, R.X. (Ed.), Geochronology and Geochemistry of Cenozoic Volcanic Rocks in China. Seismic Press, pp. 320–329 (in Chinese).

Fiorentini, M.L., Stone, W.E., Beresford, S.W., Barley, M.E., 2004. Platinum-group element alloy inclusions in chromites from Archaean mafic–ultramafic units: evidence from the Abitibi and the Agnew–Wiluna Greenstone Belts. Mineralogy and Petrology 82, 341–355.

Francis, R.D., 1990. Sulfide globules in mid-ocean ridge basalts (MORB), and the effect of oxygen abundance in Fe–S–O liquids on the ability of those liquids to partition metals from MORB and komatiite magmas. Chemical Geology 85, 199–213.

GBGMR (Guangdong Bureau of Geology and Mineral Resources), 1988. Regional Geology of Guangdong Province. Geological Publishing House, Beijing, pp. 361–387 (in Chinese).

Govindaraju, K., 1994. Compilation of working values and sample description for 383 geostandards. Geostandard Newsletter 18, 1–158.

Han, J.W., Xiong, X.L., Zhu, Z.Y., 2009. Geochemistry of Late-Cenozoic basalts from Leigiong area: the origin of EM2 and the contribution from sub-continental lithosphere mantle. Acta Petrologica Sinica 25, 3208–3220 (in Chinese with English abstract).

Handler, M.R., Bennett, V.C., 1999. Behaviour of platinum-group elements in the subcontinental mantle of eastern Australia during variable metasomatism and melt depletion. Geochimica et Cosmochimica Acta 63, 3597–3618.

Hilde, T.W.C., Uyeda, S., Kroenke, L., 1977. Evolution of the western pacific and its margin. Tectonophysics 38 (145–152), 155–165.

Ho, K.S., Chen, J.C., Juang, W.S., 2000. Geochronology and geochemistry of late Cenozoic basalts from the Leiqiong area, southern China. Journal of Asian Earth Sciences 18, 307–324.

Keays, R.R., 1995. The role of komatiitic and picritic magmatism and S-saturation in the formation of ore deposits. Lithos 34, 1–18.

Le Maitre, R.W., 1989. A Classification of Igneous Rocks and Glossary of Terms. Blackwell Scientific Publication, Oxford, p. 193.

Li, J.P., Wang, J., 2002. Mantle redox state evolution in eastern China and its implications. Acta Geologica Sinica-English Edition 76, 238–248.

Lightfoot, P.C., Keays, R.R., 2005. Siderophile and chalcophile metal variations in flood basalts from the Siberian trap, Noril'sk region: implications for the origin of the Ni–Cu–PGE sulfide ores. Economic Geology 100, 439–462.

Lightfoot, P.C., Naldrett, A.J., Gorbachev, N.S., Fedorenko, V.A., Hawkesworth, C.J., Doherty, W., 1994. Chemostratigraphy of Siberian Trap lavas Noril'sk destrict Russia: implications and source of flood basalt magmas and their associated Ni–Cu mineralization. In: Lightfoot, P.C., Naldrett, A.J. (Eds.), Proc of the Sudbury-Noril'sk symposium: Ontario Geological Survey Special Publication, 5, pp. 283–312.

Liu, C., Xie, G., Masuda, A., 1995. Geochemistry of Cenozoic basalts from eastern China (I): major element and trace element compositions, petrogenesis, and characteristics of mantle source. Geochimica 24, 1–19 (in Chinese with English abstract).

Liu, Y., Liu, H.C., Li, X.H., 1996. Simultaneous and precise determination of 40 trace elements in rock samples using ICP-MS. Geochimica 25, 552–558 (in Chinese with English abstract).

Liu, M., Cui, X., Liu, F., 2004. Cenozoic rifting and volcanism in eastern China: a mantle dynamic link to the Indo-Asian collision? Tectonophysics 393, 29–42.

Liu, Z.C., Wu, F.Y., Chu, Z.Y., Xu, X.S., 2010. Isotopic compositions of the peridotitic xenoliths from the Nushan area, Anhui Province: constraints on the age of subcontinental lithospheric mantle beneath the East China. Acta Petrologica Sinica 26, 1217–1240 (in Chinese with English abstract).

Locmelis, M., Pearson, N.J., Barnes, S.J., Fiorentini, M.L., 2011. Ruthenium in komatiitic chromite. Geochimica et Cosmochimica Acta. doi:10.1016/j.gca.2011.03.041.

Lorand, J.P., Delpech, G., Gregoire, M., Moine, B., O'Reilly, S.Y., Cottin, J.Y., 2004. Platinum-group elements and the multistage metasomatic history of Kerguelen lithospheric mantle (South Indian Ocean). Chemical Geology 208, 195–215.

Luguet, A., Lorand, J.P., Alard, O., Cottin, J.Y., 2004. A multi-technique study of platinum group element systematic in some Ligurian ophiolitic peridotites, Italy. Chemical Geology 208, 175–194.

Maier, W., Barnes, S.J., 2004. Pt/Pd and Pd/Ir ratios in mantle-derived magmas: a possible role for mantle metasomatism. South African Journal of Geology 107, 333.

Maier, W.D., Barnes, S.J., DeKlerk, W.J., Teigler, B., Mitchell, A.A., 1996. Cu/Pd and Cu/Pt of silicate rocks in the Bushveld complex: implications for platinum-group element exploration. Economic Geology 91, 1151–1158.

McDonough, W.F., Sun, S.S., 1995. The composition of the Earth. Chemical Geology 120, 223–253.

Meisel, T., Moser, J., 2004. Reference materials for geochemical PGE analysis: new analytical data for Ru, Rh, Pd, Os, Ir, Pt and Re by isotope dilution ICP-MS in 11 geological reference materials. Chemical Geology 208, 319–338.

Merkle, R.K.W., 1992. Platinum-group minerals in the middle group of chromitite layers at Marikana, western Bushveld Complex: indications for collection mechanisms and postmagmatic modification. Canadian Journal of Earth Sciences 29, 209–221.

Naldrett, A.J., 2004. Magmatic Sulfide Deposits: Geology, Geochemistry and Exploration. Springer, Heidelberg Berlin New York, pp. 334–335.

Nixon, G., Hammack, J., 1991. Metallogeny of ultramafic-mafic rocks in British Columbia with emphasis on the platinum-group elements: Ore Deposits, Tectonic and Metallogeny in the Canadian Cordillera, British Columbia, British Columbia Ministry of Energy and Mines, Paper, 4, pp. 125–161.

Northrup, C., Royden, L., Burchfiel, B., 1995. Motion of the Pacific plate relative to Eurasia and its potential relation to Cenozoic extension along the eastern margin of Eurasia. Geology 23, 719.

Orberger, B., Xu, Y., Reeves, S.J., 1998. Platinum group elements in mantle xenoliths from eastern China. Tectonophysics 296, 87–101.

Peach, C.L., Mathez, E.A., Keays, R.R., 1990. Sulfide melt silicate melt distribution coefficients for noble metals and other chalcophile elements as deduced from MORB: implications for partial melting. Geochimica et Cosmochimica Acta 54, 3379–3389.

Peck, D.C., Keays, R.R., 1990a. Geology, geochemistry and origin of platinum-group element-chromitite occurrences in the Heazlewood River Complex, Tasmania. Economic Geology 85, 765–793.
Peck, D.C., Keays, R.R., 1990b. Insights into the behavior of precious metals in primitive, S-undersaturated magmas: evidence from the Heazlewood River Complex, Tasmania. The Canadian Mineralogist 28, 553–577.
Philipp, H., Eckhardt, J.D., Puchelt, H., 2001. Platinum-group elements (PGE) in basalts of the seaward-dipping reflector sequence, SE Greenland coast. Journal of Petrology 42, 407–432.
Qi, Q.U., Taylor, L.A., Zhou, X.M., 1995. Petrology and geochemistry of mantle peridotite xenoliths from SE China. Journal of Petrology 36, 55–79.
Qi, L., Zhou, M.F., Wang, C.Y., 2004. Determination of low concentrations of platinum group elements in geological samples by ID-ICP-MS. Journal of Analytical Atomic Spectrometry 19, 1335–1339.
Rehkämper, M., Halliday, A.N., Fitton, J.G., Lee, D.C., Wieneke, M., Arndt, N.T., 1999. Ir, Ru, Pt, and Pd in basalts and komatiites: new constraints for the geochemical behavior of the platinum-group elements in the mantle. Geochimica et Cosmochimica Acta 63, 3915–3934.
Reisberg, L., Zhi, X.C., Lorand, J.P., Wagner, C., Peng, Z.C., Zimmermann, C., 2005. Re–Os and S systematics of spinel peridotite xenoliths from east central China: evidence for contrasting effects of melt percolation. Earth and Planetary Science Letters 239, 286–308.
Righter, K., Campbell, A.J., Humayun, M., Hervig, R.L., 2004. Partitioning of Ru, Rh, Pd, Re, Ir, and Au between Cr-bearing spinel, olivine, pyroxene and silicate melts. Geochimica et Cosmochimica Acta 68, 867–880.
Song, X.Y., Zhou, M.F., Keays, R.R., Cao, Z.M., Sun, M., Qi, L., 2006. Geochemistry of the Emeishan flood basalts at Yangliuping, Sichuan, SW China: implications for sulfide segregation. Contributions to Mineralogy and Petrology 152, 53–74.
Song, X.Y., Keays, R.R., Xiao, L., Qi, H.W., Ihlenfeld, C., 2009. Platinum-group element geochemistry of the continental flood basalts in the central Emeisihan Large Igneous Province, SW China. Chemical Geology 262, 246–261.
Sun, S.S., McDonough, W., 1989. Chemical and isotopic systematics of oceanic basalts: implications for mantle composition and processes: Geological Society, London, Special Publications, 42, p. 313.
Tatsumi, Y., Oguri, K., Shimoda, G., 1999. The behaviour of platinum-group elements during magmatic differentiation in Hawaiian tholeiites. Geochemical Journal 33, 237–248.
Tatsumoto, M., Basu, A.R., Wankang, H., Junwen, W., Guanghong, X., 1992. Sr, Nd, and Pb isotopes of ultramafic xenoliths in volcanic rocks of Eastern China: enriched components EMI and EMII in subcontinental lithosphere. Earth and Planetary Science Letters 113, 107–128.
Taylor, S.R., McLennan, S.M., 1985. The Continental Crust: Its Composition and Evolution. Blackwell, Oxford, p. 312.
Tredoux, M., Lindsay, N., Davies, G., McDonald, I., 1995. The fractionation of platinum-group elements in magmatic systems, with the suggestion of a novel causal mechanism. South African Journal of Geology 98, 157.
Uyeda, S., Miyashiro, A., 1974. Plate tectonics and Japanese islands: a synthesis. Geological Society of America Bulletin 85, 1159–1170.
Wang, C.Y., Zhou, M.F., Qi, L., 2011. Chalcophile element geochemistry and petrogenesis of high-Ti and low-Ti magmas in the Permian Emeishan large igneous province, SW China. Contributions to Mineralogy and Petrology 161, 237–254.
Xie, X., Xu, X.S., Zou, H.B., Xing, G.F., 2001. Trace element and Nd–Sr–Pb isotope studies of Mesozoic and Cenozoic basalts in coastal area of SE China. Acta Petrologica Sinica 17, 617–628 (in Chinese with English abstract).
Xu, Y.G., 1994. Hétérogénéité du manteau supérieur sous l'Est de la Chine: faille de Tanlu et régions adjacentes. Les enclaves des péridotites dans les basaltes cénozoïques. Université de Paris 07, Paris, p. 224 (in French).
Xu, Y.G., 1999. Continental basaltic magmatism in extensional environment: characteristics and geodynamic processes. In: Zheng, Y.F. (Ed.), Chemical Geodynamics. Science Press, Beijing, pp. 159–167.
Xu, Y.G., Orberger, B., Reeves, S.J., 1998. Fractionation of platinum group elements in upper mantle: evidence from peridotite xenoliths from Wangqing. Science in China Series D-Earth Sciences 41, 354–361 (in Chinese with English abstract).
Xu, X., O'Reilly, S.Y., Griffin, W., Zhou, X., 2003. Enrichment of upper mantle peridotite: petrological, trace element and isotopic evidence in xenoliths from SE China. Chemical Geology 198, 163–188.
Yu, J., O'Reilly, S.Y., Zhang, M., Griffin, W., Xu, X., 2006. Roles of melting and metasomatism in the formation of the lithospheric mantle beneath the Leizhou Peninsula, South China. Journal of Petrology 47, 355–383.
Zhang, X.Q., Zhou, X.P., Chen, X.Y., 1993. Atlas of Drill-core Based Cretaceous and Tertiary Stratigraphy Classification of Sanshui Basin. Ocean Press, Beijing, p. 183 (in Chinese).
Zheng, J.P., Sun, M., Zhou, M.F., Robinson, P., 2005. Trace elemental and PGE geochemical constraints of Mesozoic and Cenozoic peridotitic xenoliths on lithospheric evolution of the North China Craton. Geochimica et Cosmochimica Acta 69, 3401–3418.
Zhou, M.F., 1994. PGE distribution in 2.7-Ga layered komatiite flows from the Belingwe greenstone belt, Zimbabwe. Chemical Geology 118, 155–172.
Zhou, X., Armstrong, R.L., 1982. Cenozoic volcanic rocks of eastern China — secular and geographic trends in chemistry and strontium isotopic composition. Earth and Planetary Science Letters 58, 301–329.
Zhou, X.H., Zhu, B.Q., Liu, R.X., Chen, W.J., 1988. Cenozoic Basaltic Rocks in Eastern China, Continental Flood Basalts. Springer, p. 311.
Zhou, M.F., Sun, M., Keays, R.R., Kerrich, R.W., 1998. Controls on platinum-group elemental distributions of podiform chromitites: a case study of high-Cr and high-Al chromitites from Chinese orogenic belts. Geochimica et Cosmochimica Acta 62, 677–688.
Zhou, H.M., Xiao, L., Dong, Y.X., Wang, C.Z., Wang, F.Z., Ni, P.Z., 2009. Geochemical and geochronological study of the Sanshui basin bimodal volcanic rock suite, China: implications for basin dynamics in southeastern China. Journal of Asian Earth Sciences 34, 178–189.
Zou, H.B., Zindler, A., Xu, X.S., Qi, Q., 2000. Major, trace element, and Nd, Sr and Pb isotope studies of Cenozoic basalts in SE China: mantle sources, regional variations, and tectonic significance. Chemical Geology 171, 33–47.